

Sympathetic cooling route to Bose-Einstein condensate and Fermi-liquid mixtures

Robin Côté,¹ Roberto Onofrio,^{2,3,4} and Eddy Timmermans⁵

¹*Department of Physics, University of Connecticut, Storrs, CT 06269, USA*

²*Department of Physics and Astronomy, Dartmouth College, 6127 Wilder Laboratory, Hanover, NH 03755, USA*

³*Dipartimento di Fisica “G. Galilei”, Università di Padova, Via Marzolo 8, Padova 35131, Italy*

⁴*Center for Statistical Mechanics and Complexity, INFN, Unità di Roma 1, Roma 00185, Italy*

⁵*T-4, Theory Division, Los Alamos National Laboratory, Los Alamos, NM 87545, USA*

We discuss a sympathetic cooling strategy that can successfully mitigate fermion-hole heating in a dilute atomic Fermi-Bose mixture and access the temperature regime in which the fermions behave as a Fermi-liquid. We introduce an energy-based formalism to describe the temperature dynamics with which we study a specific and promising mixture composed of ⁶Li and ⁸⁷Rb. Analyzing the harmonically trapped mixture, we find that the favourable features of this mixture are further enhanced by using different trapping frequencies for the two species.

PACS numbers: 03.75.Ss, 05.30.Jp, 32.80.Pj, 67.90.+z

Introduction. Cold atom mixtures of fermions and Bose-Einstein condensates (BEC) [1] suggest a new venue for the study of quantum liquid mixtures that were previously available only in the form of condensed ³He-⁴He mixtures [2]. While we understand the helium phase separation to be caused by mediated interactions [3], a first-principle description of this and other helium quantities is complicated by strong interaction effects [4]. These also reduce the boson mediated interactions that can Cooper-pair [3] the ³He fermions, giving a critical temperature T_c currently inaccessible. Mediated interactions and their prominence near a quantum phase transition (quantum criticality, see [5]) have also been identified as the probable cause of the observed non-Fermi-liquid behavior in high T_c superconductors [5] and, perhaps, of high T_c superconductivity itself. In these systems, however, a clear understanding is again impeded by the ambiguity of experimental data.

The above issues [6] can be studied in a much cleaner and more accessible environment when cold atom physicists succeed in cooling fermion-boson mixtures into the Fermi-liquid regime [2] in which the fermions behave in a universal manner that follows from expanding the energy to second order in quasi-particle occupation numbers. This implies a heat capacity that varies linearly with temperature, a feature that often serves as experimental test of Fermi-liquid behavior. In a dilute fermion gas, it sets in below ten percent of the Fermi temperature $T < 0.1T_F$, whereas $T < 0.02T_F$ is required in the ³He liquid. For cold atom quantum liquid studies, which can also access fermion-boson mixtures in a parameter regime that is fundamentally different from that of the helium mixtures [7], crossing into the Fermi-liquid regime is as crucial of a step as cooling below T_c is for the study of superfluidity. So far, experiments that use bosons to cool fermion atoms (sympathetic cooling) have not entered this regime [8] because the low temperature drop in the BEC heat capacity impairs its ability to refrigerate [9], and because the unavoidable loss of fermions leads

to significant heating [10]. The BEC introduces further losses in the Fermi system (three-body recombinations) thereby increasing the Fermi-hole heating rate.

In this Rapid, we show that with a large boson-to-fermion mass ratio and with the proper trapping parameters, sympathetic cooling *can* access the Fermi-liquid temperature regime. Heavy bosons require many collisions from the lighter fermions before they heat significantly. The corresponding increase in BEC heat capacity is crucial; low three-body recombination rates are helpful. The need to strike a delicate balance between keeping the fermion boson overlap sufficiently low to reduce hole-heating, but sufficiently high to ensure efficient fermion-BEC heat exchange can be met by adjusting the fermion and boson trapping frequencies in a bichromatic trapping scheme. We illustrate these points for the promising candidate of a ⁶Li-⁸⁷Rb mixture, which has been recently experimentally investigated [11].

Loss-induced Temperature Dynamics. - The cold atom many-body states of interest are metastable (the true ground state being a condensed solid) and trapped atom gases have a finite lifetime. Atoms leave the trap as a consequence of collisions with room temperature background atoms, of two-body spin relaxation processes (in magnetic traps), and of three-body recombination. Instead of describing the many-body response to particle loss, we keep track of the energy-balance and define the effective temperature of the system T as the temperature at which an equilibrium system with the same number of particles has the same energy.

The above collisions reduce the number of particles of type j , N_j , as well as internal energy E , as each loss removes the energy of the lost particles. If the collision products, on their way out of the trap, collide with the remaining atoms, the process also adds an average kinetic energy ϵ_j^{coll} . We equate the total energy balance rate, $dE/dt - \sum_j \epsilon_j^{coll} dN_j/dt$ to the variation of the total equilibrium energy of a temperature-relaxed system, $dE(N_j, T)/dt = (\partial E/\partial T)dT/dt + \sum_j (\partial E/\partial N_j)dN_j/dt$

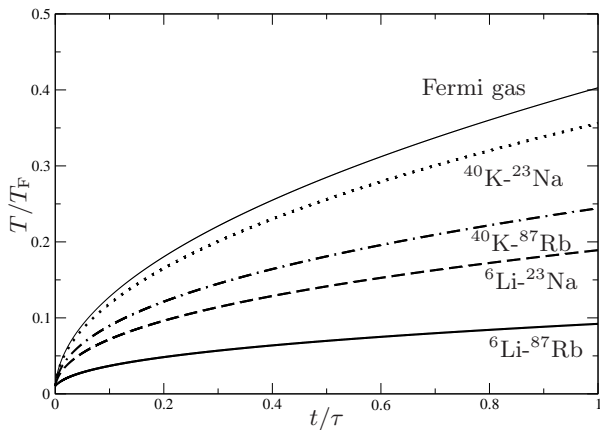


FIG. 1: Hole heating in homogeneous Fermi-Bose mixtures. The temperature, T , scaled by the Fermi temperature, T_F , is depicted for four Fermi-Bose mixtures consisting of fermionic ${}^6\text{Li}$ or ${}^{40}\text{K}$ atoms with ${}^{23}\text{Na}$ or ${}^{87}\text{Rb}$ as bosonic partners, starting at $T/T_F = 10^{-2}$. For comparison, the hole heating curve for pure fermions, assuming the same loss-rate, is also plotted (lighter continuous curve).

and we identify the usual thermodynamic derivatives, $(\partial E/\partial T) = C$, where C denotes the heat capacity at constant number of particles, and $(\partial E/\partial N_j) = \mu_j$, where μ_j represents the chemical potential of the j -particles. Equating the energy rates and solving for the temperature derivative, we obtain the central equation of temperature dynamics

$$\frac{dT}{dt} = \frac{1}{C} \left(\frac{dF}{dt} - \sum_j \epsilon_j^{\text{coll}} \frac{dN_j}{dt} \right), \quad (1)$$

where we have defined F as the free energy that occurs in Fermi-liquid theory: $F = E - \sum_j \mu_j N_j$ (here dependent on N_j rather than μ_j).

Homogeneous ideal gas Fermi-Bose mixtures. - The homogeneous mixture of a single component degenerate fermion gas and a BEC allows a transparent description of hole heating and its mitigation by sympathetic cooling. Apart from border effects, the homogeneous mixture can be realized by using blue-detuned laser light sheets [12]. Atoms in the mixture undergo various three-body loss processes. For instance, a fermion can recombine with a boson into a highly energetic molecule while ejecting a second boson, corresponding to

$$\dot{n}_B = -2\alpha n_B^2 n_F, \quad \dot{n}_F = -\alpha n_B^2 n_F \quad (2)$$

where n_F and n_B represent the fermion and boson densities respectively, and α denotes the three-body loss rate coefficient. Processes involving three-boson collisions do not lead to significant heating and those involving two or three indistinguishable fermions are Pauli-inhibited. If, as in Eq. (2), the rate is energy-insensitive, the loss of one out of N_F fermions removes, on average, a kinetic energy

$\frac{3}{5}E_F$, where E_F is the Fermi energy. At the same temperature the remaining degenerate system of $N_F - 1$ fermions would have an energy E_F less than the initial Fermi system of N_F fermions. The net result is an effective energy increase of $\frac{2}{5}E_F$ per fermion lost (assuming, optimistically, $\epsilon_j^{\text{coll}} = 0$). We apply Eq. (1) to the homogeneous mixture of fermions of mass m_F , and an ideal BEC of N_B bosons of mass m_B . The total heat capacity of an ideal or near-ideal gas mixture is the sum of the BEC and fermion heat capacities, $C = k_B N_F (\pi^2/2) (T/T_F) [1 + (45/8\pi^{3/2}) \zeta_{5/2}(1) (m_B/m_F)^{3/2} \sqrt{T/T_F}]$, where k_B denotes the Boltzmann constant, T_F is the Fermi-temperature, $T_F = E_F/k_B$ and $\zeta_{5/2}(1) = 1.342$. The time scale of the dynamics is the lifetime τ of the fermion system, $\tau^{-1} = \alpha n_B^2$,

$$\frac{d(T/T_F)}{d(t/\tau)} = \frac{\frac{4}{5\pi^2} \left(\frac{T}{T_F}\right)^{-1}}{1 + \frac{45\zeta_{5/2}(1)}{8\pi^{3/2}} \left(\frac{m_B}{m_F}\right)^{3/2} \left(\frac{T}{T_F}\right)^{1/2}}. \quad (3)$$

The term $\propto \sqrt{T/T_F}$ in the denominator stems from the BEC heat capacity and represents its capability to absorb heat released from fermion-hole heating. Note the sensitive dependence on mass-ratio illustrated by Fig. 1, where the temperature of mixtures that start out at $T = 0.01T_F$ is shown for four possible Fermi-Bose mixtures with stable alkalis (${}^6\text{Li}$ or ${}^{40}\text{K}$ for the fermionic species, ${}^{23}\text{Na}$ or ${}^{87}\text{Rb}$ for the bosonic species). For the sake of comparison, we recover the fermion-hole heating rate for a pure fermion system obtained in Ref. [10] by setting $m_B \rightarrow 0$, corresponding to a BEC-refrigerator of vanishing heat capacity (shown by the thin full line).

Trapped interacting mixtures. - In addition to the mass-ratio dependence, the spatial density profiles in the realistic case of trapped gases affect the temperature dynamics. The fermion-boson overlap can be reduced by a repulsive inter-species interaction or by the occurrence of a true phase separation. In the non-phase separated systems, the mutual overlap can be controlled by varying the ratio of the fermion to boson trapping frequencies (using, for instance, a bichromatic trap [9]). A decrease in overlap reduces fermion loss but also reduces the efficiency of sympathetic cooling. Which effect wins out, depends sensitively on the density profiles and, hence, on the interaction parameters.

To determine the trap densities in the case of a ${}^6\text{Li}$ - ${}^{87}\text{Rb}$ mixture, the most promising candidate shown in Fig. 1, we have evaluated the interspecies elastic scattering lengths for various Li and Rb isotopes. Although spectroscopic data for LiRb potential curves are lacking, the excellent agreement between *ab initio* [13] and our parametrized potentials (see Table I) at large separation attest to the accuracy of the curves in that region. However, there is a discrepancy between both sets of curves near the equilibrium distance. Compared to [13] our potential curves are deeper by about 3% for the singlet and

	s	${}^6\text{Li}-{}^{87}\text{Rb}$	${}^6\text{Li}-{}^{85}\text{Rb}$	${}^7\text{Li}-{}^{87}\text{Rb}$	${}^7\text{Li}-{}^{85}\text{Rb}$
a_T	1.0	-43.6	-36.6	-151	-118
	0.99280	-17.0	-12.9	-60.0	-48.7
	0.97404	+17.0	+18.8	+5.43	+8.43
a_S	1.0	+153	+215	-16.3	-1.11
	0.99280	-152	-77.4	+27.1	+33.8
	0.97404	+45.5	+50.4	+167	+280

TABLE I: Singlet and triplet elastic scattering lengths (shifted and unshifted) for the mixtures of Li and Rb isotopes, in Bohr radii. The values of s are found so that $a_T = \pm 17 a_0$, and the same scaling was assumed for the singlet. The scattering lengths were obtained from potential curves with *ab initio* data from [15], joined smoothly to an exponential wall of the form ce^{-bR} at short separations R , and to the long-range form $-C_6/R^6 - C_8/R^8 - C_{10}/R^{10} \mp AR^\alpha e^{-\beta R}$ at $R=13.5 a_0$. Here, \mp stands for the singlet $X^1\Sigma^+$ and triplet $a^3\Sigma^+$ molecular states, respectively. The values for $C_6 = 2545$ a.u. from [16], and $C_8 = 2.34 \times 10^5$ a.u. and $C_{10} = 2.61 \times 10^7$ a.u. from [17], were used. The parameters of the exchange energy are $\alpha = 4.9417$ a.u. and $\beta = 1.1836$ a.u. [18], while the constant $A = 0.0058$ a.u. was found by fitting the *ab initio* data.

7% for the triplet channel. By scaling the whole potential curves so that $V_s(R) = sV(R)$ with $s \leq 1$, we can explore the effect of having shallower potential curves; the values of the scattering lengths change significantly as s varies accordingly. In the singlet case, one bound level disappears, and the scattering length varies between $\pm\infty$, while the triplet scattering length becomes positive. Recently, Zimmermann and co-workers [11] determined the magnitude of the triplet scattering length of ${}^6\text{Li}-{}^{87}\text{Rb}$ to be $|a_T| = 17_{-6}^{+9} a_0$. In Table I, we present values for the singlet and triplet scattering lengths for the unshifted ($s = 1$) and shifted potentials (so that a_T agrees with $\pm 17 a_0$). These values as well as those calculated in [14] are tentative and future measurements are required to specify the potentials more accurately. Such experimental feedback can be obtained from either one of the isotopes so that we list the results for all combinations, regardless of their fermionic or bosonic nature.

We now study the temperature of a ${}^6\text{Li} - {}^{87}\text{Rb}$ mixture trapped in an idealized trap: both species are contained by cylindrical trapping potentials $V_F(\mathbf{r})$ and $V_B(\mathbf{r})$ that are of the hard wall type in the transverse direction with the same radius R_T , where R_T is much larger than the BEC healing length and the average fermion-fermion distance. In the longitudinal direction, the fermions and bosons experience harmonic trapping potentials with different trapping frequencies ω_f and ω_b respectively. Apart from its simplicity, such a situation reproduces the relevant heating features of a generic three-dimensional cold atom mixture with anisotropic confinement. From Table I, we find that some hyperfine states of the ${}^6\text{Li}$ and ${}^{87}\text{Rb}$ isotopes that can be trapped magnetically give positive valued inter-species scattering lengths, thereby favoring spatial separation in the trap. The density profiles $n_B(\mathbf{r})$

and $n_F(\mathbf{r})$ in a Thomas-Fermi approximation are determined by (see Molmer reference in [6])

$$n_B(\mathbf{r}) = \frac{\mu_B - V_B(\mathbf{r}) - \lambda_{FB}n_F(\mathbf{r})}{\lambda_B}$$

$$n_F(\mathbf{r}) = \frac{[2m_F]^{3/2}}{6\pi^2\hbar^3} \{\mu_F - V_F(\mathbf{r}) - \lambda_{FB}n_B(\mathbf{r})\}^{3/2} \quad (4)$$

where λ_B and λ_{FB} denote the boson-boson and fermion-boson interaction strengths proportional to the corresponding s -wave scattering lengths, a_B and a_{FB} : $\lambda_B = 4\pi\hbar^2 a_B/m_B$ and $\lambda_{FB} = 2\pi\hbar^2 a_{FB} (1/m_F + 1/m_B)$. In Eq. (4), we tacitly assume temperature independent density profiles, a good approximation in the regime of interest. Solving Eq. (4) numerically, we find that a decrease in confinement strength for the bosons generally increases the overlap with the Fermi species. Controlling the relative trapping frequencies allows for a variation of the fermion-boson overlap and, hence, the rate of Fermi-hole heating and the efficiency of sympathetic cooling. The effect of inter-species interactions is marginal on the Fermi gas but is very pronounced for the BEC, and the mutual overlap is very sensitive to the interaction parameters. The temperature trajectories shown in Fig. 2 are calculated for $\omega_f = 10^3 \text{ s}^{-1}$, while varying the Bose trap frequency as shown in the caption. We choose the chemical potentials in the initial state to be $1 \mu\text{K}$ for the Fermi gas and 100 nK for the Bose gas. The scattering lengths are chosen as $a_B = 5.8 \text{ nm}$ for Rb and $a_{FB} = -0.90 \text{ nm}$ for the Li-Rb interactions.

We consider the fermions to be subject to loss by background scattering, $\dot{n}_F(x) = -\gamma n_F(x)$, as well as by the 3-body recombination of Eq. (2). While these loss-rates are unknown, we have chosen values that corresponded to $\gamma = 10 \text{ Hz}$ and $\tau_3^{-1} = \alpha n_B^2 = 4 \text{ s}^{-1}$ at the peak densities of case $\omega_f/\omega_b = 1$ of Fig. 2. The behavior shown in Fig. 2 is quite robust with respect to various choices of the relevant parameters. In addition, we assumed that a continued evaporative cooling of the bosons drains away energy from the system at a realistic rate. In the calculations with different fermion and boson trapping frequencies, we took the evaporative cooling rates to be equal and accounted for the low overlap drop in evaporative cooling efficiency by introducing a figure of merit as described in Ref. [19]. This allows to introduce an effective evaporative cooling rate $-\dot{Q}_{\text{eff}}$ proportional to the overlap of the two clouds. The rate of free energy change is then identified as sum of three terms: $dF/dt = (dF/dt)_{3b} + (dF/dt)_{\text{Bkgnd}} - \dot{Q}_{\text{eff}}$, where the free energy rates have to be calculated from the resulting density profiles,

$$\left(\frac{dF}{dt}\right)_{3b} = \frac{(6\pi^2)^{2/3}\hbar^2\alpha}{5m_F} \int d^3r [n_F(\mathbf{r})]^{5/3} [n_B(\mathbf{r})]^2, \quad (5)$$

whereas as in [10], the background scattering free energy

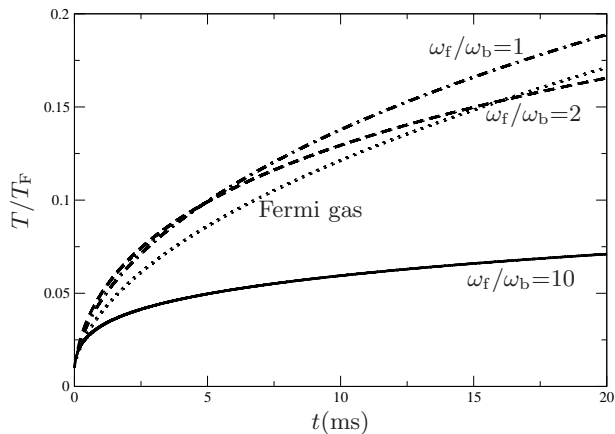


FIG. 2: Fermi hole heating of harmonically trapped ${}^6\text{Li}$ - ${}^{87}\text{Rb}$ mixtures. The dependence of the degeneracy parameter T/T_F (starting from an initial value of $T/T_F = 10^{-2}$) on time is depicted for three cases of $\omega_f/\omega_b = 1$ (dot-dashed curve), $\omega_f/\omega_b = 2$ (dashed), $\omega_f/\omega_b = 10$ (continuous). The dotted curve represents the intrinsic Fermi hole heating for the same loss-rate of the fermions but in the absence of the ${}^{87}\text{Rb}$ atoms.

increase rate is given by

$$\left(\frac{dF}{dt}\right)_{\text{Bkgnd}} = \frac{3(6\pi^2)^{2/3}\hbar^2\gamma}{10m_F} \int d^3r [n_F(\mathbf{r})]^{5/3}. \quad (6)$$

Finally, the temperature trajectory follows from Eq. (1), in which we use Eqs. (5) and (6)

$$\frac{dT}{dt} = \frac{(dF/dt)_{3b} + (dF/dt)_{\text{Bkgnd}} - \dot{Q}_{\text{eff}}}{C_F(T) + C_B(T)}, \quad (7)$$

where C_F and C_B denote the fermion and boson heat capacities. The resulting temperature dynamics is depicted in Fig. 2 for three different trapping frequency ratios. These results show that the heating rate is mitigated best by using a larger ω_f/ω_b -ratio, at least until the spatial overlap is decreased due to an excessive spreading of the Bose cloud.

Conclusion. - Our study of loss-induced heating, based on an effective equilibration model, reveals that a cold atom Fermi-Bose mixture of high boson to fermion mass ratio such as ${}^6\text{Li}$ - ${}^{87}\text{Rb}$ can be maintained in the Fermi liquid temperature regime. This result, a consequence of the increased BEC heat capacity due to the larger trapping frequency ratio between fermions and bosons, could open up a new avenue for cold atom studies. We also discuss a specific cooling strategy which could be soon implemented in the experimental investigations going on for the specific ${}^6\text{Li}$ - ${}^{87}\text{Rb}$ mixture, for which anomalous heating has been observed [11].

R.C. acknowledges partial support from NSF, R.O. from Cofinanziamento MIUR, and E.T. from the Los Alamos Laboratory Directed Research and Development (LDRD) program.

- [1] M. W. Zwierlein *et al.*, Phys. Rev. Lett. **92**, 120403 (2004); T. Bourdel *et al.*, Phys. Rev. Lett. **93**, 050401 (2004); G. Modugno *et al.*, Science **297** 2240 (2002); R. Hulet, presentation in the Quantum Gas Conference at the Kavli Institute for Theoretical Physics, Santa Barbara, CA, May 10-14 (2004).
- [2] G. Baym and C. Pethick, *Landau Fermi-liquid theory*, (Wiley, 1991).
- [3] J. Bardeen, G. Baym, and D. Pines, Phys. Rev. Lett. **17**, 372 (1966).
- [4] E. Krotscheck and M. Saarela, Phys. Rep. **232**, 1 (1993).
- [5] G. R. Stewart, Rev. Mod. Phys. **73**, 797 (2001).
- [6] Cold atom fermion-BEC mixtures are expected to undergo phase separation, as discussed in L. Viverit, C. J. Pethick, and H. Smith, Phys. Rev. A **61**, 053605 (2000), and trapped phase separated systems can exhibit a variety of spatial arrangements as shown by K. Molmer, Phys. Rev. Lett. **80**, 1804 (1998). The prospect of Cooper-pairing induced by BEC mediated interactions was treated by H. Heiselberg *et al.*, Phys. Rev. Lett. **85**, 2418 (2000). If the attractive Yukawa interaction that follows from the static perturbation treatment (see, for instance, M. J. Bijlsma, B. A. Heringa, and H. T. C. Stoof, Phys. Rev. A **61**, 053601 (2000)), is valid then the formation of Cooper pairs that are smaller than the Yukawa range is similar to that of excitons in exciton BECs, see, for instance, P. Nozieres, and D. Saint James, J. Physique **43**, 1133 (1982). Magnetic instabilities of spinor BECs or phase separation of a BEC-mixture can provide a quantum phase transition in cold atom fermion-BEC mixtures.
- [7] Cold atom single component fermion-BEC mixtures with a Fermi-velocity v_F that exceeds the BEC sound velocity c , exhibit zero-sound as well as BEC-sound collective excitations, whereas $v_F < c$ -mixtures (the regime of helium liquid mixtures) only exhibit BEC-sound, as shown in D. H. Santamore, S. Gaudio, and E. Timmermans, Phys. Rev. Lett. **93**, 250402 (2004).
- [8] A. G. Truscott *et al.*, Science **291**, 2570 (2001); F. Schreck *et al.*, Phys. Rev. Lett. **87**, 080403 (2001); Z. Hadzibabic *et al.*, Phys. Rev. Lett. **88**, 160401 (2002); **91**, 160401 (2003); G. Roati *et al.*, Phys. Rev. Lett. **89**, 150403 (2002).
- [9] R. Onofrio and C. Presilla, Phys. Rev. Lett. **89**, 100401 (2002); J. Stat. Phys. **115**, 57 (2004).
- [10] E. Timmermans, Phys. Rev. Lett. **87**, 240403 (2001).
- [11] C. Silber *et al.*, e-print cond-mat/0506217 (9 June 2005).
- [12] N. Davidson *et al.*, Phys. Rev. Lett. **74**, 1311 (1995).
- [13] B. O. Roos (private communication).
- [14] H. Ouerdane and M. J. Jamieson, Phys. Rev. A **70**, 022712 (2004).
- [15] M. Korek *et al.*, Chem. Phys. **256**, 1 (2000).
- [16] A. Derevianko, J. F. Babb, and A. Dalgarno, Phys. Rev. A **63**, 052704 (2001).
- [17] S. G. Porsev and A. Derevianko, J. Chem. Phys. **119**, 844 (2003).
- [18] B. M. Smirnov and M. I. Chibisov, Sov. Phys. JETP **21**, 624 (1965).
- [19] M. Brown-Hayes and R. Onofrio, Phys. Rev. A **70**, 063614 (2004).